

Photocatalytic Decomposition of Alkylsiloxane Self-Assembled Monolayers on Titanium Oxide Surfaces

Jae P. Lee, Hee K. Kim, Chan R. Park, Gyoosoon Park, Hyon T. Kwak, Sang M. Koo,[†] and Myung. M. Sung*

Department of Chemistry, Kookmin University, Chongnung-dong, Songbuk-ku, Seoul 136-702, Korea and Department of Industrial Chemistry, College of Engineering, Hanyang University, Seoul 133-791, Korea

Received: January 22, 2003; In Final Form: May 12, 2003

The photocatalytic decomposition of octadecyltrichlorosilane (OTS) based self-assembled monolayer formed on TiO₂ has been studied using atomic force microscopy (AFM), X-ray photoelectron spectroscopy (XPS), and contact angle analysis. The TiO₂ thin films were grown on Si(100) substrates by atomic layer deposition from titanium isopropoxide and water. Densely packed alkylsiloxane monolayers similar in quality to those on SiO₂ are formed on TiO₂. It is found that the monolayers on TiO₂ are decomposed much faster than those on SiO₂ under UV irradiation of 254 nm in air. The OTS-based SAMs on TiO₂ are decomposed through the photocatalytic oxidation of the alkyl chains with a gradual and homogeneous reduction in chain length. After the complete photodecomposition of the OTS-SAMs, the siloxane headgroups remain on the TiO₂ surface. The observation indicates that the titanium oxide, a well-known photocatalyst for organic pollutant treatment, efficiently decomposes the alkylsiloxane monolayers under UV irradiation in air.

I. Introduction

Self-assembled monolayers (SAMs) are thin organic films which form spontaneously on solid surfaces. They have been shown to be useful as passivating layers and also for the modification of surface properties. Potential applications include wetting, adhesion, friction, chemical sensing, ultrafine scale lithography, and protection of metals against corrosion.^{1–3} Several different varieties of SAMs have been investigated, including alkanethiols (CH₃(CH₂)_{n-1}SH) on Au, Ag, and Cu, and alkyltrichlorosilanes (CH₃(CH₂)_{n-1}SiCl₃) on SiO₂, Al₂O₃, and mica.¹

SAMs have considerable potential as high-resolution resists for ultrafine scale lithography. Because of their small intermolecular distance of less than 1 nm, their potential resolution is higher than for polymer resists. High-resolution patterns can be formed by decomposing or removing SAMs using electron beams,⁴ ion beams, photolithography,⁵ or scanning probe microscopy.⁶ Among various patterning methods, photolithography is most practical, since it can transfer an entire pattern on a photomask to a SAM at a single time. The photolithography with alkanethiol SAMs has been done to have submicrometer spatial resolution. It is suggested that photogenerated ozone attacks the thiolate headgroups to produce cleavage of the C–S bond.⁷ There have been a few reports on UV photopatterning of alkylsiloxane SAMs in air. However, previous studies have shown that the UV photopatterning of the alkylsiloxane SAMs requires relatively large amounts of energy, since they are quite stable to UV irradiation of 254 nm, as compared to alkanethiolate SAMs.⁸ The alkylsiloxane SAMs are slowly decomposed through the photooxidation of the alkyl chains by OH radical and atomic oxygen produced from the dissociation of photo-generated ozone under UV irradiation in air.

It is therefore of particular interest to find an effective way for photodecomposition of the alkylsiloxane SAMs. Considering its effectiveness for the photocatalytic decomposition of organic compounds,^{9–11} TiO₂ photocatalysis can be a promising way to decompose the alkylsiloxane SAMs and ultimately applicable to UV photopatterning of them. Upon UV irradiation of 254 nm, the semiconductor TiO₂ can generate electron–hole pairs and subsequently produce highly reactive oxygen species (e.g., OH, O₂ radicals) via electron scavenging by adsorbed O₂ and hole trapping by the surface OH⁻ or adsorbed H₂O.^{12–14} These oxygen radicals can oxidize and decompose most organic compounds and some inorganic compounds. So far, few studies have been concerned with the photocatalytic decomposition of the monolayers on TiO₂ photocatalyst. Haick and Paz¹⁵ have observed that the monolayers on TiO₂ film are effectively decomposed under UV irradiation by using in-situ FT-IR analysis. In this research, we study morphological changes of the alkylsiloxane SAMs and reaction intermediates during the monolayer photodecomposition on TiO₂ thin films by using atomic force microscopy, X-ray photoelectron spectroscopy, and contact angle analysis. Particular attention is focused on the mechanism of the photodecomposition of the monolayers. It is found that the monolayers are rapidly and homogeneously decomposed on the TiO₂ films under UV irradiation in air through the photooxidation of the alkyl chains, resulting in loss of carbon and uniform decrease in the monolayer height.

II. Experimental Section

Preparation of Si Substrates. The Si substrates used for TiO₂ film growth in this research were cut from n-type (100) wafers with resistivity in the range 1–5 Ωcm. The Si substrates were initially treated by a chemical cleaning process, which involves degreasing, HNO₃ boiling, NH₄OH boiling (alkali treatment), HCl boiling (acid treatment), rinsing in deionized water, and blow-drying with nitrogen, proposed by Ishizaka and Shiraki¹⁶ to remove contaminants. A thin protective oxide layer was

* To whom correspondence should be addressed. E-mail: smm@kookmin.ac.kr; phone: 011-82-2-910-4767; fax: 011-82-2-910-4415.

[†] Hanyang University.

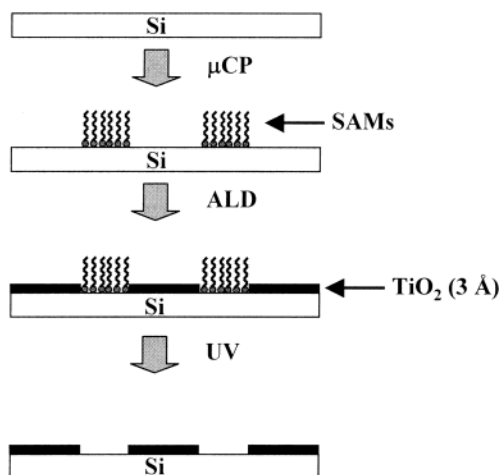


Figure 1. Preparation scheme of patterned TiO_2 thin film on Si substrate.

grown on the Si substrate by chemical oxidation with peroxy-sulfuric acid.

Preparation of TiO_2 Thin Films. The Si substrates were introduced into the atomic layer deposition (ALD) system Cyclic 4000 (Genitech, Teajon, Korea). The TiO_2 thin films were deposited onto the Si substrates using $\text{Ti}(\text{OCH}(\text{CH}_3)_2)_4$ (STREM Chemicals) and water as ALD precursors. Ar gas served both as a carrier and a purging gas. The $\text{Ti}(\text{OCH}(\text{CH}_3)_2)_4$ and water were evaporated at 80 and 20 °C, respectively. The number of ALD cycles in a run was kept 400. The cycle consisted of 2 s exposure to $\text{Ti}(\text{OCH}(\text{CH}_3)_2)_4$, 5 s to Ar purge, 2 s to water, and 5 s to Ar purge. The total flow rate of the Ar gas was 20 sccm. The TiO_2 thin films were grown at 200 °C under 2 Torr. The thickness of the TiO_2 films, measured by transmission electron microscopy (TEM, JEOL), is about 150 Å.

Preparation of Patterned TiO_2 Thin Films. Patterned TiO_2 thin films on the Si substrate were made by using microcontact printing and atomic layer deposition (Figure 1). The Si substrate surface was patterned with OTS-based SAMs by microcontact printing. A poly(dimethylsiloxane) (PDMS) stamp having 2.5- μm parallel lines and 3.5- μm spaces was fabricated according to a previously reported procedure.^{17–19} The PDMS stamp was inked with a 10 mM hexane solution of OTS and dried with nitrogen. The stamp was placed in contact on the Si substrate for 30 s. The stamp was carefully peeled off and the substrate was blown dry with nitrogen. A TiO_2 thin film was selectively deposited onto the SAMs-patterned Si substrate by ALD. The number of ALD cycles in a run was kept 10. The thickness of the TiO_2 films, measured by AFM, is about 3 Å.

Preparation of OTS-Based SAMs. Alkylsiloxane SAMs were formed by immersing the TiO_2 film samples in a 2.5 mmol solution of octadecyltrichlorosilane (OTS) precursor dissolved in hexadecane–chloroform (4:1). The samples were then washed in carbon tetrachloride to remove excess reactants and dried with nitrogen. For comparison, the monolayers were also formed on SiO_2 thin films, prepared by chemical oxidation of the Si(100) substrates with peroxy-sulfuric acid.

Photodecomposition of the OTS-Based SAMs. Immediately after the samples were prepared, the SAMs-coated samples were introduced into a controlled environmental chamber with a Oriel 450 W Xe lamp (UV Enhanced) with total intensity of 5 mW/cm^2 at a working distance of 10 cm. The primary wavelength of the lamp is 254 nm. Relative humidity was kept in all experiments at 40%.

Analysis Techniques. Atomic force microscopy images of the samples were obtained on a PSI CPII operating in tapping

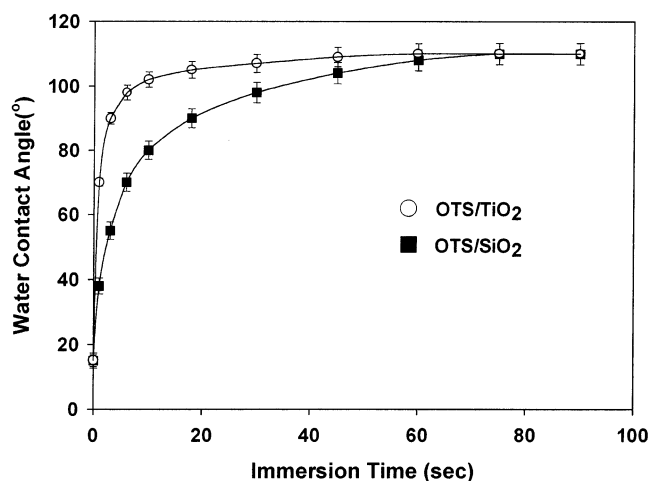


Figure 2. Water contact angle of the TiO_2 and SiO_2 samples as a function of immersion time in OTS solution.

mode. The X-ray photoelectron spectroscopy (XPS) measurements were conducted using the ESCALAB MKII. Water contact angles of the film samples were determined on a model A-100 Rame-Hart NRL goniometer in the ambient air by using the sessile drop method.

III. Results and Discussion

A. Formation of OTS-Based SAMs on TiO_2 and SiO_2 .

Figure 2 shows changes in the water contact angle of the TiO_2 and SiO_2 samples as a function of immersion time in OTS solution. The contact angle of the TiO_2 rapidly increases and is close to the limiting value after ~ 40 s of immersion, whereas that of the SiO_2 reaches the plateau after ~ 75 s. The final water contact angle of the TiO_2 sample is about 112° in good agreement with the value measured on the SiO_2 sample. The ratio of $\text{C}(1s)/[\text{Si}(2p) + \text{Ti}(2p)]$ peak area measured by XPS is similar for both the OTS-coated TiO_2 and SiO_2 , which is consistent with the contact angle data suggesting that the monolayers are similar in quality on both surfaces. Monolayer formation was quenched by removing the TiO_2 and SiO_2 samples from the OTS solution after 1 and 7 s, respectively. At this point, both partial monolayers consist of islands (~ 24 Å high) of closely packed, fully extended chains, as shown by the AFM images in Figure 3. The water contact angle and the $\text{C}(1s)/[\text{Si}(2p) + \text{Ti}(2p)]$ peak area ratio for both partial monolayers are about 65° and 0.5, respectively. These values indicate that the partial monolayers have an OTS coverage of approximately 30% in respect to full monolayers. The OTS islands on the SiO_2 sample are more branched and larger than those on the TiO_2 sample. These observations suggest that the monolayers are similar in quality on both samples, whereas the surface reactivity for the OTS adsorption on both samples is different.

According to the formation mechanism of the alkylsiloxane monolayers, the OTS molecules in the organic solvent can be gradually adsorbed onto a water layer present on SiO_2 .²⁰ Following physisorption, the trichlorosilane head groups are hydrolyzed to form trisilanols. Recently, we proved that the silanols exist in a highly mobile hydrogen-bonded state.²¹ This leads to important in-plane reorganizations of OTS molecules, thereby forming a uniform densely packed molecular island at the early stage of monolayer formation on the SiO_2 substrate. Silanol head groups of this island then become grafted to the SiO_2 substrate by irreversible cross-linking to one another and covalent grafting to the substrate surface. On the other hand, the grafting on the TiO_2 substrate is expected faster than that

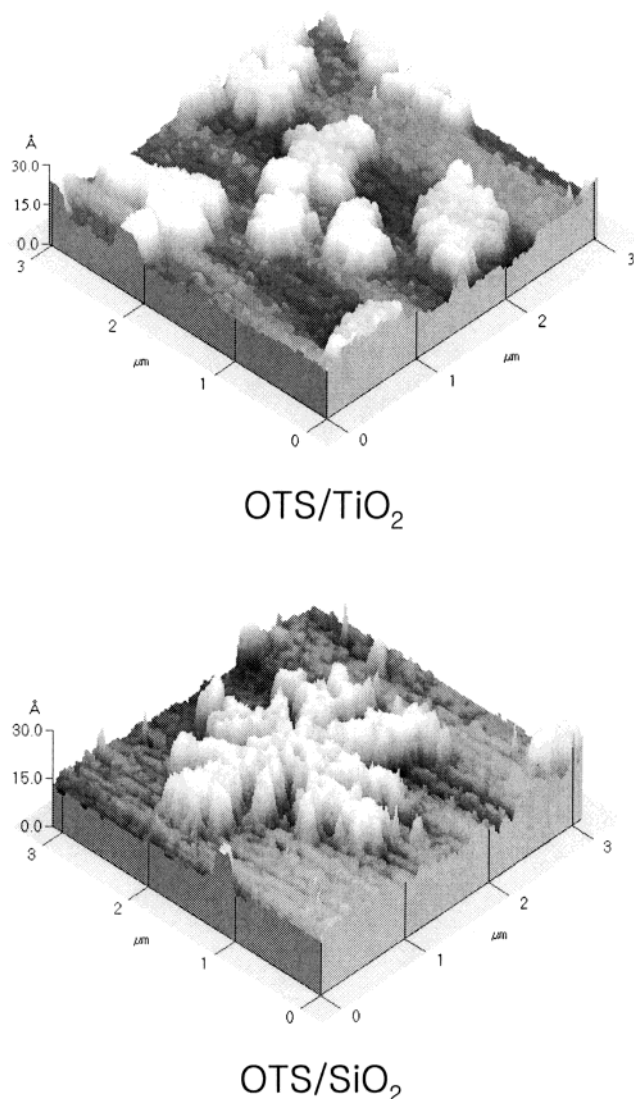


Figure 3. AFM image of a partial OTS-based monolayer grown on the TiO_2 and SiO_2 samples for 7 s.

on the SiO_2 because the condensation rate of the silanols with hydroxyl groups on the TiO_2 surface is faster than that on the SiO_2 surface because of a higher electronegativity of titanium. The chemical reactivity of metal hydroxide toward condensation depends mainly on the electronegativity of the metal atom.²² Therefore, the grafting reaction on the TiO_2 surface is much faster than that on the SiO_2 . Since the island formation of the OTS molecules requires lateral mobility hindered by the fast grafting reaction on the TiO_2 surface, the OTS islands are smaller on the TiO_2 as can be seen in Figure 3.

B. Photodecomposition of OTS-Based SAMs on TiO_2 and SiO_2 . The water contact angle and XP peak intensities for OTS-based SAMs on the TiO_2 and SiO_2 samples were measured as a function of UV irradiation time in air. Figure 4 shows that the contact angle of the monolayers on the TiO_2 rapidly declines with UV irradiation, whereas that on the SiO_2 slowly decreases. The C(1s) peak intensity for the SAMs on the TiO_2 also rapidly decreases with UV irradiation, but the Si(2p) peak intensity slightly increases and reaches the plateau after 2 min of UV irradiation (Figure 5). The decomposition rate of the monolayers on the TiO_2 is 20 times faster than that on SiO_2 . These observations suggest that the TiO_2 film efficiently decomposes alkyl chains of the OTS-based SAMs with UV irradiation in

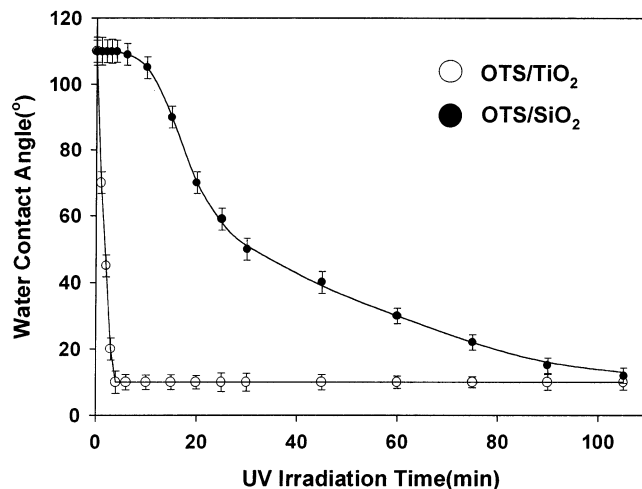


Figure 4. Water contact angle as a function of UV irradiation time for the OTS-based SAMs on the TiO_2 and SiO_2 .

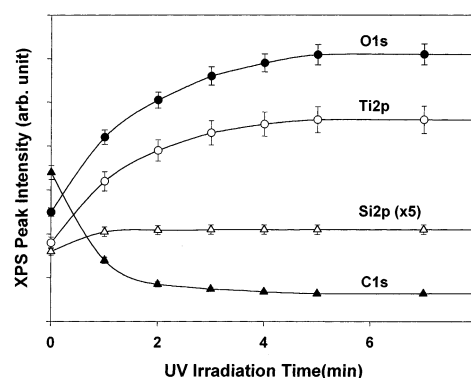


Figure 5. XP peak intensities as a function of UV irradiation time for the OTS-based SAMs on the TiO_2 .

air but that the siloxane head groups remain on the TiO_2 surface during the monolayer photodecomposition.

To study the mechanism of photodecomposition of the OTS-based SAMs on TiO_2 , the partial monolayer on TiO_2 , prepared as just described, was analyzed by AFM with increasing UV irradiation time. The obtained AFM images and cross sections are displayed in Figure 6. After the partial monolayer is irradiated for 1 min, the height of the SAM islands is uniformly reduced to 15 Å. The size and shape of the islands remain intact, suggesting that the island perimeter does not display enhanced reactivity. There is no evidence for growth of the pinholes within these islands. After irradiation for 3 min, the height has been reduced to about 8 Å. After 4 min, almost no islands are present. All these results indicate that the alkyl chains of OTS-SAMs on TiO_2 are gradually and homogeneously reduced in chain length. High-resolution spectra of the C(1p) peak for the OTS-based SAMs on TiO_2 are shown in Figure 7 as a function of UV irradiation time in air. The spectra show that with UV irradiation, the C(1s) peak at 284.6 eV decreases in intensity and new peaks appear at 286.2 and 288.6 eV. The C(1s) peak at 284.6 eV is assigned to alkyl species, while the peaks at 286.2 and 288.6 eV are assigned to alkoxy and carbonyl species, respectively.²³ These observations suggest that oxygenated hydrocarbon intermediates are formed during the photodecomposition of the OTS-based SAMs on TiO_2 .

Previous studies have shown that the alkylsiloxane monolayers on SiO_2 are slowly decomposed by OH radical and atomic oxygen generated from UV dissociation of ozone.⁸ A photodecomposition mechanism of the alkylsiloxane monolayers on SiO_2 is suggested on the basis of the mechanism of gas-phase

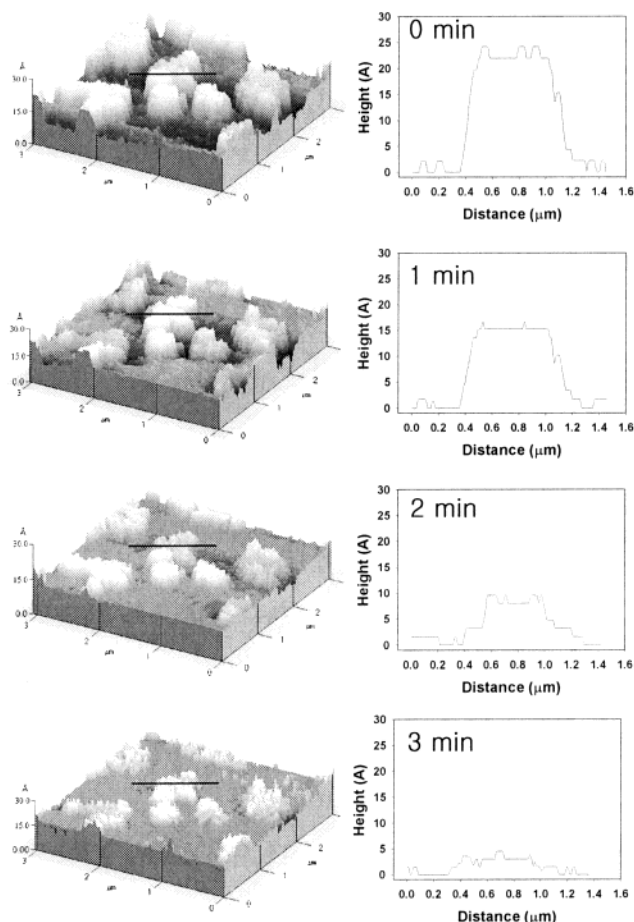


Figure 6. AFM images and cross sections as a function of UV irradiation time for the partial OTS-based monolayer on the TiO₂.

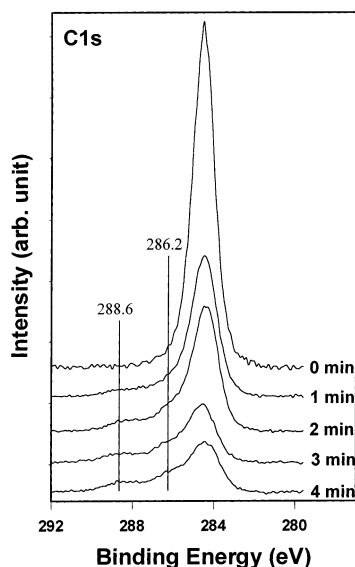


Figure 7. XP high-resolution spectra of the C(1s) regions as a function of UV irradiation time for the partial OTS-based monolayer on the TiO₂.

oxidation of alkanes.²⁴ An initiation step is hydrogen abstraction from alkyl chains by attacks of OH radical and atomic oxygen, thereby forming alkyl radicals. The alkyl radicals further react to form alkoxy radicals, which can be oxidized to form carbonyls. The resulting carbonyls dissociate via direct photolysis or attack from radicals with loss of carbon, thus reducing the length of alkyl chains. The similar mechanism can be

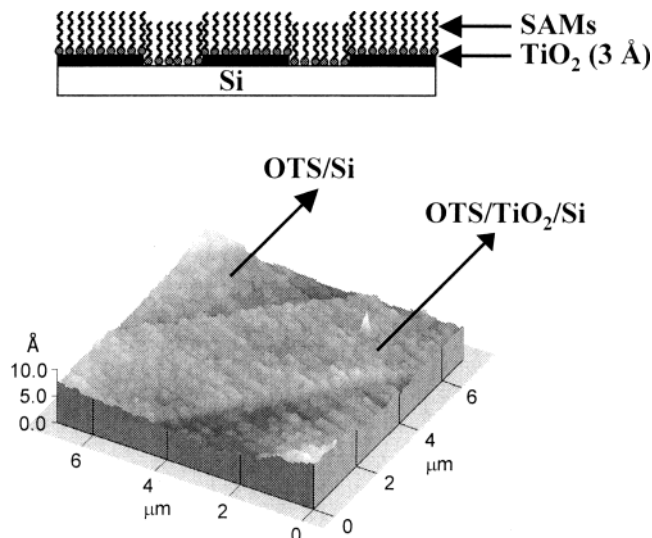


Figure 8. Scheme and AFM image of the OTS-based monolayer on the patterned TiO₂ thin film.

applicable to the photodecomposition of the OTS-based SAMs on TiO₂ in this study. First, the reactive oxidizing species (e.g., $\cdot\text{OH}$, $\text{O}_2^{\cdot-}$, $\cdot\text{OOH}$ radicals) generated on the TiO₂ surface under UV irradiation abstract hydrogen atoms from the alkyl chains of SAMs. The continuous attacks of the oxidizing species to alkyl radicals produce alkoxy radicals and carbonyls. The resulting alkoxy radicals and carbonyls on the TiO₂ surface are further decomposed via successive photocatalysis and then form shorter alkyl chains with loss of carbon. The XPS results in Figure 7 confirm that oxygenated hydrocarbon intermediates such as alcohols and carbonyls are formed because of the attacks of oxygen radicals to alkyl radicals during the continuous photodecomposition. The OTS-based SAMs on the TiO₂ surface are decomposed much faster than those on the nonconductor SiO₂ because the semiconductor TiO₂ as a photocatalyst can more efficiently produce active oxygen radicals (e.g., $\cdot\text{OH}$, $\text{O}_2^{\cdot-}$, $\cdot\text{OOH}$) by UV irradiation in air.

On the other hand, the photogeneration mechanisms of active oxygen radicals are different between SiO₂ and TiO₂. In SiO₂ system, active oxygen radicals are generated via UV dissociation of ozone photogenerated from air. However, TiO₂ generates active oxygen radicals on its surface via reactions of photogenerated electrons and holes with surface-adsorbed species such as water and oxygen by UV irradiation in air. To explain the gradual reduction in a monolayer height on TiO₂, it is needed that active oxygen radicals diffuse from the TiO₂ surface to the end of alkyl chains of OTS-based monolayer.

C. Photodecomposition of OTS-Based SAMs on Patterned TiO₂/Si. To investigate the mechanism of the generation and diffusion of reactive oxidizing species (e.g., $\cdot\text{OH}$, $\text{O}_2^{\cdot-}$, $\cdot\text{OOH}$ radicals) on the OTS-coated TiO₂, the OTS-based SAMs have been formed on patterned TiO₂ thin films on the Si substrate, as shown in Figure 9. Since the thickness of the TiO₂ films, measured by AFM, is about 3 Å, the height of the OTS-based monolayer on the patterned TiO₂ domains is 3 Å higher than that on the Si stripes. AFM images of the monolayer were obtained as a function of UV irradiation time. AFM images and cross sections are displayed in Figure 9. After 2 min irradiation, the height of the OTS monolayer on the TiO₂ domains is uniformly reduced by 12 Å and thus becomes much lower than that on the Si stripes. This result reveals that the OTS monolayer on the TiO₂ domains is decomposed much faster than that on the Si stripes during the first 2 min of irradiation. The size and shape of the monolayer remains intact and there

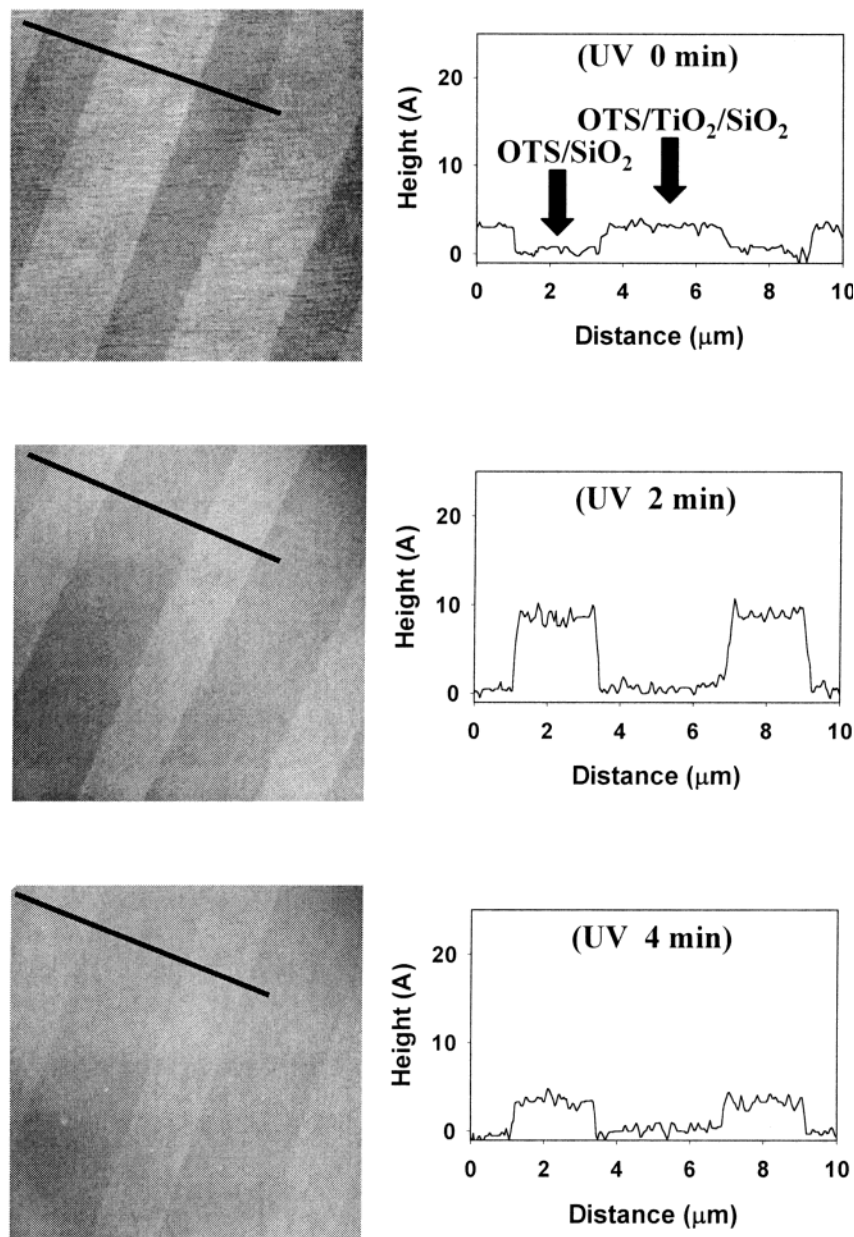


Figure 9. AFM image and cross sections as a function of UV irradiation time for the OTS-based SAMs on the patterned TiO₂ thin film.

is no evidence for growth of the pinholes found within the monolayer. After 4 min irradiation, the height of the monolayer on the Si stripes is also reduced with uniform morphological changes such as that on the TiO₂ stripes.

All these results indicate that the OTS-based monolayer on the TiO₂ domains is primarily and rapidly decomposed at the beginning of irradiation because oxidizing species are generated on the surface of UV-irradiated TiO₂. At prolonged irradiation, the OTS monolayer on the Si domains becomes decomposed following the photodecomposition on the TiO₂ domains because it takes time for oxidizing species photogenerated on the TiO₂ surface to reach and attack the OTS chains on the Si domains. This remote photodecomposition of the OTS monolayer on the Si domains can be explained by surface migration or diffusion of photogenerated oxidizing species (e.g., $\cdot\text{OH}$, $\text{O}_2^{\cdot-}$, $\cdot\text{OOH}$ radicals) from the TiO₂ domains to the OTS chains on the Si domains, as previously reported.¹⁵ At prolonged irradiation, the OTS chains on the TiO₂ domains become much shorter than those on the Si domains, probably enhancing the diffusion of

oxidizing species from the TiO₂ domains to the OTS chains on the Si domains.

IV. Conclusions

The photodecomposition of alkylsiloxane self-assembled monolayers on the TiO₂ and SiO₂ thin films has been studied using atomic force microscopy (AFM), X-ray photoelectron spectroscopy (XPS), and contact angle analysis. The OTS-based SAMs on TiO₂ are similar in quality to those on SiO₂, whereas the surface reactivity for the OTS adsorption on both samples is different. The OTS-based SAMs are more efficiently and rapidly decomposed on the TiO₂ surface with UV irradiation in air, as compared to those on the SiO₂. Our studies of the OTS-based SAMs on TiO₂ with UV irradiation reveal that the monolayers decompose through the photocatalytic oxidation of the alkyl chains with a gradual reduction in chain length. The reactive oxidizing species (e.g., $\cdot\text{OH}$, $\text{O}_2^{\cdot-}$, $\cdot\text{OOH}$ radicals) generated on the TiO₂ surface under UV irradiation abstract hydrogen atoms from the alkyl chains of the monolayers. The

resulting alkyl radicals on the TiO₂ surface are continuously attacked by the reactive oxidizing species, producing alkoxy radicals and carbonyls, and then form shorter alkyl radicals with loss of carbon. After the complete photodecomposition of the OTS-SAMs, the siloxane headgroups remain on the TiO₂ surface.

Acknowledgment. This work was supported by a program of National Research Laboratory from the Ministry of Science and Technology and a grant No.(R01-2001-000-00047-0) from Korea Science & Engineering Foundation.

References and Notes

- (1) Ulman, A. *An Introduction to Ultrathin Organic Films*; Academic Press: Boston, MA, 1991.
- (2) Swalen, J. D.; Allara, D. L.; Andrade, J. D.; Chandross, E. A.; Garoff, S.; Israelachvili, J.; McCarthy, T. J.; Murray, R.; Pease, R. F.; Rabolt, J. F.; Wynne, K. J.; Yu, H. *Langmuir* **1987**, *3*, 932.
- (3) Jennings, G. K.; Laibinis, P. E. *Colloids Surf., A* **1996**, *116*, 105.
- (4) Carr, D. W.; Lercel, M. J.; Whelan, C. S.; Craighead, H. G.; Seshadri, K.; Allara, D. L. *J. Vac. Sci. Technol., A* **1997**, *15*, 1446.
- (5) Huang, J. Y.; Hemminger, D. A. *Langmuir* **1994**, *10*, 626.
- (6) Xu, S.; Liu, G. *Langmuir* **1997**, *13*, 127.
- (7) Poirier, G. E.; Herne, T. M.; Miller, C. C.; Tarlov, M. J. *J. Am. Chem. Soc.* **1999**, *121*, 9703.
- (8) Tao, Y.; Wynn, D.; Dudek, R.; Borguet, E. *Langmuir* **2001**, *17*, 4497.
- (9) *Photocatalysis Fundamentals and Applications*; Serpone, N., Pelizzetti, Eds.; Wiley: Amsterdam, 1989.
- (10) *Photocatalytic Purification and Treatment of Water and Air*; Ollis, D. F., Al-Ekabi, Eds.; Elsevier: Amsterdam, 1993.
- (11) Fuhishima, A.; Honda, K. *Nature* **1972**, *238*, 37.
- (12) Ishibashi, K.; Nosaka, Y.; Hashimoto, K.; Fujishima, A. *J. Phys. Chem. B* **1998**, *102*, 2118.
- (13) Saka, T.; Kawai, T. *Chem. Phys. Lett.* **1981**, *80*, 341.
- (14) Turchi, C. S.; Ollis, D. F. *J. Catal.* **1990**, *122*, 178.
- (15) Haick, H.; Paz, Y. *J. Phys. Chem. B* **2001**, *105*, 3045.
- (16) Ishizaka, A.; Shiraki, Y. *J. Electrochem. Soc.* **1986**, *133*, 666.
- (17) Kumar, A.; Whitesides, G. M. *Appl. Phys. Lett.* **1993**, *63*, 2002.
- (18) Kumar, A.; Biebuyck, H.; Whitesides, G. M. *Langmuir* **1994**, *10*, 1498.
- (19) Wilbur, J. L.; Kumar, A.; Kim, E.; Whitesides, G. M. *Adv. Mater.* **1994**, *6*, 600.
- (20) Brzoska, J. B.; Ben Azouz, I.; Rondelez, F. *Langmuir* **1994**, *10*, 4367.
- (21) Sung, M. M.; Carraro, C.; Yauw, O. W.; Kim, Y.; Maboudian, R. *J. Phys. Chem.* **2000**, *104*, 1556.
- (22) Brinker, C. J.; Scherer, G. W. *Sol-Gel Science*; Academic Press: New York, 1990.
- (23) Briggs, D.; Seah, M. P. *Practical Surface Analysis*; John Wiley & Sons Ltd.: England, 1990.
- (24) Cox, R.; Patrick, K.; Chant, S. *Environ. Sci. Technol.* **1981**, *15*, 587.